JOURNAL OF GUIDANCE, CONTROL, AND DYNAMICS
Vol. 29, No. 2, March–April 2006

Nonlinear Aeroelastic System Identification with Application to Experimental Data

Sunil L. Kukreja* and Martin J. Brenner†
NASA Dryden Flight Research Center, Edwards, California 93523-0273

Representation and identification of a nonlinear aeroelastic pitch–plunge system as a model of the NARMAX class is considered. A nonlinear difference equation describing this aircraft model is derived theoretically and shown to be of the NARMAX form. Identification methods for NARMAX models are applied to aeroelastic dynamics and their properties demonstrated via continuous-time simulations of experimental conditions. Simulation results show that 1) the outputs of the NARMAX model closely match those generated using continuous-time methods and 2) NARMAX identification methods applied to aeroelastic dynamics provide accurate discrete-time parameter estimates. Application of NARMAX identification to experimental pitch–plunge dynamics data gives a high percent fit for cross-validated data.

I. Introduction

SYSTEM identification or mathematical modeling is the process of developing or improving a mathematical representation of a physical system based on observed data. System identification is a critical step in aircraft development, analysis, and validation for flight-worthiness.

One such application of system identification in the aerospace/flight-test community is the analysis of aeroelasticity. Aeroelasticity is concerned with the interaction of inertia with structural, and aerodynamic forces.[1] Previous approaches have modeled aeroelasticity with linear time-invariant (LTI) models.[2] These linear models have been successful in providing approximate estimates of an aircraft's response to gust, turbulence, and external excitations.[3] However, when aircraft speeds increase to high subsonic or transonic Mach numbers, linear models no longer provide accurate predictions of the aircraft's behavior. Some of the behavior that cannot be modeled linearly includes transonic dip, airflow separation, and shock oscillations, which can induce nonlinear phenomena such as limit cycle oscillations (LCO)[4,5]: The onset of LCOs has been observed on several aircraft such as the F-16C and F/A-18 and cannot be modeled properly as a LTI system.[6] This has necessitated the application of nonlinear identification techniques to accurately model LCO dynamics.

Over the past several decades, significant achievements have been made in several areas of non-parametric nonlinear system identification (see, e.g., Refs. 7–9). Recent work in the aerospace community has attempted to address these nonlinear aeroelastic phenomena using Volterra kernel methods.[10] These methods provide a convenient means of characterizing LCOs but suffer from a highly over-parameterized model description and do not lend themselves to efficient control synthesis.

Parametric representations of nonlinear systems typically contain a small number of coefficients, which can be varied to alter the behavior of the equation and may be linked to the underlying system. Leontaritis and Billings[11,12] have proposed the NARMAX (nonlinear autoregressive moving average exogenous) structure as a general parametric form for modeling nonlinear systems. NARMAX models describe nonlinear systems in terms of linear-in-the-parameters difference equations relating the current output to (possibly nonlinear) combinations of inputs and past outputs. It is suitable for modeling both the stochastic and deterministic components of a system and is capable of describing a wide variety of nonlinear systems.[13,14] This formulation yields compact model descriptions that may be readily identified and may afford greater interpretability. NARMAX models have been successfully demonstrated for modeling the input–output behavior of many complex systems such as ones found in engineering and biology.[15,16] The NARMAX model class offers an ideal framework for describing nonlinear behavior such as aeroelastic aircraft dynamics.

Currently, development and testing of aircraft take many years and considerable expenditure of limited resources. One reason for lengthy development time and high costs is that many models (and hence control strategies) need to be developed throughout the flight envelope. The power of parametric nonlinear identification techniques (i.e., NARMAX models) is that they can describe complex aeroelastic behavior over a large operating range. Consequently, they provides models that can be more robust and reduce development time.

Although the NARMAX structure is well suited to modeling the input–output behavior of a aeroelastic system, to date it has not been investigated by the flight-test community. Therefore, in this paper, we 1) theoretically analyze a nonlinear pitch–plunge model of aircraft dynamics to derive its NARMAX representation, 2) assess the applicability of this nonlinear model for the identification of aerospace systems, and 3) investigate the suitability of NARMAX identification methods applied to aircraft dynamics.

Our results show that the NARMAX model class provides an ideal framework for modeling the input–output behavior of a nonlinear pitch–plunge model describing aircraft dynamics. Identification results illustrate that methods for identification of NARMAX models are well suited for identifying aircraft dynamics. Analysis of experimental data using NARMAX identification techniques provides a parameter set that explains the input–output data well. Overall, this paper contributes to the understanding of the use of parametric identification techniques for modelling of aerospace systems.

The organization of this paper is as follows. The NARMAX model structure is described in Section II. In Section III a continuous-time representation of a nonlinear pitch–plunge model describing aircraft dynamics is given, and its NARMAX representation is derived in Section IV. Section V illustrates the results of simulating this NARMAX representation of pitch–plunge dynamics. In Section VI the applicability of NARMAX identification to this model representation is assessed via simulations of experimental conditions. Section VII presents the results of identifying experimental wind tunnel data, and Section VIII provides a discussion of the major findings. Last, in Section IX conclusions and significance of the results are given.

Received 21 December 2004; revision received 14 March 2005; accepted for publication 5 April 2005.

*National Research Council Research Associate, MailStop 4840 D, Structural Dynamics Group, Aerospace Branch; sunil.kukreja@nasa.gov.

†Research Engineer, MailStop 4840 D, Structural Dynamics Group, Aerospace Branch.

II. NARMAX Model

The NARMAX (nonlinear autoregressive, moving average exogenous) structure is a general parametric form for modeling nonlinear systems.[11] This structure describes both the stochastic and deterministic components of nonlinear systems. Many nonlinear systems are a special case of the general NARMAX structure.[14] The NARMAX structure models the input–output relationship as a nonlinear difference equation of the form

$$z(n) = f^l[z(n-1), \ldots, z(n-n_y), u(n), \ldots, u(n-n_u), e(n-1), \ldots, e(n-n_e)] + e(n) \quad (1)$$

f^l denotes a nonlinear mapping, u is the controlled or exogenous input, z is the measured output, and e is the uncontrolled input or innovation. The nonlinear mapping, f^l, can be described by a wide variety of nonlinear functions such as $\tanh(\cdot)$ or splines (i.e., hard nonlinearities).[13,14] For simplicity, nonlinearities only that can be described by a polynomial expansion are considered. This class of nonlinear difference equations describes the dynamic behavior of a system as a linear and/or nonlinear expansion of the input, output and error. It may include a variety of nonlinear terms, such as terms raised to an integer power (e.g., $u^3(n-5)$), products of present and past inputs (e.g., $u(n)u(n-3)$), past outputs (e.g., $y^2(n-2)y(n-7)$), or cross-terms (e.g., $u(n-3)y^2(n-4)$). This system description encompasses many forms of nonlinear difference equations that are linear in the parameters. Thus, there are no problems with local minima.

III. Nonlinear Pitch–Plunge Model of Aircraft Dynamics

O'Neil and Strganac[17] and O'Neil et al.[18] developed a nonlinear pitch–plunge model (Fig. 1) describing aircraft aeroelastic dynamics. Figure 1 characterizes aeroelastic wing dynamics for experiments performed on the Texas A&M testbed.[18] This model provides a relationship between control surface deflection as input and pitch–plunge displacement and velocity as outputs of a single-input multiple-output nonlinearity followed by a simple integrator.

The model presented in Fig. 1 has been derived from the governing equations of motion for aeroelastic systems as

$$\begin{bmatrix} m & mx_\alpha b \\ mx_\alpha b & I_\alpha \end{bmatrix}\begin{bmatrix} \ddot{h} \\ \ddot{\alpha} \end{bmatrix} + \begin{bmatrix} c_h & 0 \\ 0 & c_\alpha \end{bmatrix}\begin{bmatrix} \dot{h} \\ \dot{\alpha} \end{bmatrix} + \begin{bmatrix} k_h & 0 \\ 0 & k_\alpha(\alpha) \end{bmatrix}\begin{bmatrix} h \\ \alpha \end{bmatrix} = \begin{bmatrix} -L \\ M \end{bmatrix} \quad (2)$$

where h denotes plunge motion, α pitch angle, x_α nondimensional distance between elastic axis and center of mass, m wing mass, I_α mass moment of inertia of the wing about the elastic axis, b semichord of the wing, $\{c_h, c_\alpha\}$ plunge and pitch structural damping coefficients, $\{k_h, k_\alpha\}$ plunge and pitch structural spring constants, and L, M aerodynamic lift and moment.

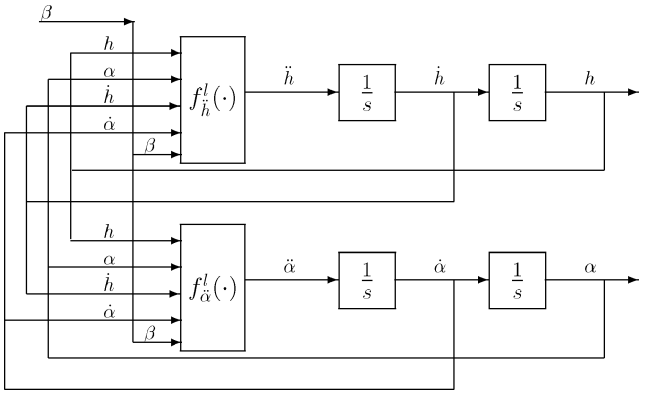

Fig. 1 System structure assumed for modeling and identification of pitch–plunge aeroelastic dynamics.

Typically, quasi-steady aerodynamic forces and moments are assumed, which can be modeled as

$$L = \rho U^2 b c_{l_\alpha}\left[\alpha + \dot{h}/U + \left(\tfrac{1}{2} - a\right)b(\dot{\alpha}/U)\right] + \rho U^2 b c_{l_\beta}\beta$$

$$M = \rho U^2 b^2 c_{m_\alpha}\left[\alpha + \dot{h}/U + \left(\tfrac{1}{2} - a\right)b(\dot{\alpha}/U)\right] + \rho U^2 b^2 c_{m_\beta}\beta \quad (3)$$

where ρ denotes density of air, U freestream velocity, c_{m_α} and c_{l_α} moment and lift coefficients per angle of attack, c_{m_β} and c_{l_β} moment and lift coefficient per control surface deflection, and a nondimensional distance from midchord to elastic axis.

Although several classes of nonlinear mappings for stiffness contributions, $k_\alpha(\alpha)$, have been investigated for open loop dynamics of aeroelastic systems,[19–22] the work of O'Neil et al.[17,18] demonstrated that a polynomial mapping of the form

$$k_\alpha(\alpha) = k_{\alpha_0} + k_{\alpha_1}\alpha + k_{\alpha_2}\alpha^2 + k_{\alpha_3}\alpha^3 + k_{\alpha_4}\alpha^4 \quad (4)$$

describes the behavior of this testbed well.

Equations of motion are derived by combining Eqs. (2) and (3) to yield

$$\begin{bmatrix} m & mx_\alpha b \\ mx_\alpha b & I_\alpha \end{bmatrix}\begin{bmatrix} \ddot{h} \\ \ddot{\alpha} \end{bmatrix} + \begin{bmatrix} c_h + \rho U b c_{l_\alpha} & \rho U b^2 c_{l_\alpha}\left(\frac{1}{2} - a\right) \\ \rho U b^2 c_{m_\alpha} & c_\alpha - \rho U b^3 c_{m_\alpha}\left(\frac{1}{2} - a\right) \end{bmatrix} \times \begin{bmatrix} \dot{h} \\ \dot{\alpha} \end{bmatrix} + \begin{bmatrix} k_h & \rho U^2 b c_{l_\alpha} \\ 0 & -\rho U^2 b^2 c_{m_\alpha} + k_\alpha(\alpha) \end{bmatrix}\begin{bmatrix} h \\ \alpha \end{bmatrix} = \begin{bmatrix} -\rho b c_{l_\beta} \\ \rho b^2 c_{m_\beta} \end{bmatrix} U^2\beta \quad (5)$$

The model form presented in Fig. 1 is derived by transforming Eq. (5) to give

$$\dot{\boldsymbol{x}} = \boldsymbol{f}_\mu(\boldsymbol{x}) + \boldsymbol{g}(\boldsymbol{x})\mu\beta \quad (6)$$

where $\boldsymbol{x} = [x_1 \;\; x_2 \;\; x_3 \;\; x_4]^T = [h \;\; \alpha \;\; \dot{h} \;\; \dot{\alpha}]^T$, $\mu = U^2$, and

$$\boldsymbol{f}_\mu = \begin{bmatrix} x_3 \\ x_4 \\ -k_1 x_1 - (k_2\mu + p(x_2))x_2 - c_1 x_3 - c_2 x_4 \\ -k_3 x_1 - (k_4\mu + q(x_2))x_2 - c_3 x_3 - c_4 x_4 \end{bmatrix}$$

$$\boldsymbol{g}(\boldsymbol{x}) = \begin{bmatrix} 0 \\ 0 \\ g_3 \\ g_4 \end{bmatrix} \quad (7)$$

The supplementary variables k_i, $i = 1, 2, 3, 4$ and g_j, $j = 3, 4$ are provided in Table 1 in relationship to the aeroelastic parameters given in Eqs. (2) and (3).

Transformation of Eq. (5) to Eq. (6) and introduction of supplementary variables (Table 1) provides the simple model description presented in Fig. 1. The nonlinear mappings for this model description are given as

$$\begin{aligned} f^l_{\ddot{\alpha}}(\cdot) &= -k_3 h(n)\left[k_4\mu(m/d)\left(k_{\alpha_0} + k_{\alpha_1}\alpha + k_{\alpha_2}\alpha^2 + k_{\alpha_3}\alpha^3 + k_{\alpha_4}\alpha^4\right)\right]\alpha(n) - c_3\dot{h}(n) - c_4\dot{\alpha}(n) + g_4\mu U(n) \\ &= -b_1 h(n) - \left[b_2\alpha(n) + b_3\alpha^2(n) + b_4\alpha^3(n) + b_5\alpha^4(n) + b_6\alpha^5(n)\right] - b_7\dot{h}(n) - b_8\dot{\alpha}(n) + b_9 U(n) \\ &= \ddot{\alpha}(n) \end{aligned} \quad (8)$$

$$\begin{aligned} f^l_{\ddot{h}}(\cdot) &= -k_1 h(n) - \left[k_2\mu + (-mx_\alpha b/d)\left(k_{\alpha_0} + k_{\alpha_1}\alpha + k_{\alpha_2}\alpha^2 + k_{\alpha_3}\alpha^3 + k_{\alpha_4}\alpha^4\right)\right]\alpha(n) - c_1\dot{h}(n) - c_2\dot{\alpha}(n) + g_3\mu U(n) \\ &= -a_1 h(n) - \left[a_2\alpha(n) + a_3\alpha^2(n) + a_4\alpha^3(n) + a_5\alpha^4(n) + a_6\alpha^5(n)\right] - a_7\dot{h}(n) - a_8\dot{\alpha}(n) + a_9 U(n) \\ &= \ddot{h}(n) \end{aligned} \quad (9)$$

Table 1 Supplementary system variables

Supplementary variable	Relationship to system parameters
d	$m\left(I_\alpha - mx_\alpha^2 b^2\right)$
k_1	$I_\alpha k_h/d$
k_2	$\left(I_\alpha \rho b c_{l_\alpha} + mx_\alpha b^3 \rho c_{m_\alpha}\right)\big/d$
k_3	$-mx_\alpha b k_h/d$
k_4	$\left(-mx_\alpha b^2 \rho c_{l_\alpha} - m\rho b^2 c_{m_\alpha}\right)\big/d$
c_1	$\left[I_\alpha\left(c_h + \rho U b c_{l_\alpha}\right) + mx_\alpha \rho U b^3 c_{m_\alpha}\right]\big/d$
c_2	$\left[I_\alpha \rho U b^2 c_{l_\alpha}\left(\frac{1}{2} - a\right) - mx_\alpha b c_\alpha + mx_\alpha \rho U b^4 c_{m_\alpha}\left(\frac{1}{2} - \alpha\right)\right]\big/d$
c_3	$\left(-mx_\alpha b c_h - mx_\alpha \rho U b^2 c_{l_\alpha} - m\rho U b^2 c_{m_\alpha}\right)\big/d$
c_4	$\left[mc_\alpha - mx_\alpha \rho U b^3 c_{l_\alpha}\left(\frac{1}{2} - a\right) - m\rho U b^3 c_{m_\alpha}\left(\frac{1}{2} - a\right)\right]\big/d$
g_3	$\left(-I_\alpha \rho b c_{l_\beta} - mx_\alpha b^3 \rho c_{m_\beta}\right)\big/d$
g_4	$\left(mx_\alpha b^2 \rho c_{l_\beta} + m\rho b^2 c_{m_\beta}\right)\big/d$
$p(x_2)$	$(-mx_\alpha b/d)k_\alpha(x_2)$
$q(x_2)$	$(m/d)k_\alpha(x_2)$

Note this system (Fig. 1) can be described in terms of pitch–plunge displacement or velocity. Here pitch–plunge is chosen in terms of velocity because 1) it offers a model description with lower dynamic order and 2) velocity feedback models are often used for vibration suppression.

Many methods exist for discretization of continuous-time systems/signals. Most commonly used are Euler's forward, Euler's backward, or Tustin's method (also known as the bilinear transformation method); see, e.g., Refs. 23, 24. Each has its advantages as well as disadvantages. Although Tustin's and Euler's backward methods provide a superior approximation to a continuous-time signal, the goal in system identification is not (directly) signal reproduction but model estimation.

Tustin's method provides excellent signal estimation but its use for modeling a pure integrator yields system descriptions that can be overly complex, e.g., having redundant terms. Euler's backward method also provides good signal estimation but provides a model that is not intuitive. Models based on this approximation would include the current output as one of the model terms, leading to an algebraic loop. Although Euler's forward method is well known to be unstable, this is only true if the sampling rate is not sufficiently small. For identification purposes this does not pose a concern because the signals need to be sampled "at least" twice Nyquist and, hence, stability is achieved. Generally, the rule of thumb is to sample a signal at least 4–10 times the highest known (or suspected) system dynamics.[25] For the pitch–plunge system under investigation, Euler's forward method provides a model description that is both stable and intuitive. Moreover, all three methods converge to similar accuracies for sufficiently small sampling rates. For these reasons Euler's forward method is chosen to model the system dynamics.

IV. Theoretical Analysis

The pitch–plunge model is given in continuous time. This section shows how the model can be converted to discrete time and rewritten as a NARMAX model. To do so, note that the two nonlinearities can be decoupled and analyzed separately because they yield two separate model descriptions for pitch and plunge velocity.

Euler's forward (explicit) method[23]

$$\frac{1}{s} = \dot{x}(0) + \int_0^t \ddot{x}(t)\,\mathrm{d}t \approx \dot{x}(n-1) + T\ddot{x}(n-1) \qquad (10)$$

where T is the sample time, was used to approximate the continuous-time integrator, where $\ddot{x}$ is replaced by $\ddot{\alpha}$ and $\ddot{h}$ for pitch and plunge, respectively.

The nonlinearities used for this analysis to derive an input–output model of pitch and plunge weregiven in Eqs. (8) and (9). In addition, the models are assumed to be corrupted by output additive (measurement) noise as

$$\dot{\alpha}(n) = \dot{\alpha}_{\mathrm{nf}}(n) + e_{\dot{\alpha}}(n), \qquad \dot{h}(n) = \dot{h}_{\mathrm{nf}}(n) + e_{\dot{h}}(n) \qquad (11)$$

where $\dot{\alpha}(n)$ and $\dot{h}(n)$ are the noise-corrupted outputs, $\dot{\alpha}_{\mathrm{nf}}(n)$ and $\dot{h}_{\mathrm{nf}}(n)$ the unmeasured noise-free outputs, and $e_{\dot{\alpha}}(n)$ and $e_{\dot{h}}(n)$ the measurement noise.

After collecting terms and combining, the overall nonlinear models were represented as nonlinear difference equations with 10 terms each as

$$\begin{aligned}\dot{\alpha}(n) &= \gamma_1\dot{\alpha}(n-1) + \gamma_2 h(n-1) + \gamma_3\alpha(n-1) + \gamma_4\alpha(n-1)^2 \\ &\quad + \gamma_5\alpha(n-1)^3 + \gamma_6\alpha(n-1)^4 + \gamma_7\alpha(n-1)^5 + \gamma_8\dot{h}(n-1) \\ &\quad + \gamma_9 u(n-1) + \gamma_{10} e_{\dot{\alpha}}(n-1) \\ \dot{h}(n) &= \theta_1\dot{h}(n-1) + \theta_2 h(n-1) + \theta_3\alpha(n-1) + \theta_4\alpha(n-1)^2 \\ &\quad + \theta_5\alpha(n-1)^3 + \theta_6\alpha(n-1)^4 + \theta_7\alpha(n-1)^5 + \theta_8\dot{\alpha}(n-1) \\ &\quad + \theta_9 u(n-1) + \theta_{10} e_{\dot{h}}(n-1)\end{aligned} \qquad (12)$$

These are NARMAX models because 1) they include input–output terms that are combinations of linear and nonlinear integer powers and 2) they are linear in the parameters. Table 2 shows the relationship of discrete-time NARMAX parameters in (12) to the underlying continuous-time coefficients.

V. Validation of NARMAX Pitch–Plunge Model

The accuracy of this system representation was validated by simulating the pitch–plunge model in continuous time using Simulink (Fig. 1). The nonlinearities used in this continuous-time simulation were the fifth-order power series described in Eqs. (8) and (9). The parameters used in the simulation were typical values found in experiments and are given in Table 3 (Ref. 17). The system was excited using a 5-Hz chirp input.

A. Output Accuracy

To determine the validity of this NARMAX description model (12), its response is simulated for a parameter set corresponding to those used for the continuous-time model. The input sequence was a 5-Hz chirp with a signal duration of 30 s. The chirp input had an operating range between ± 1.0 rad (see upper panel of Fig. 2).

Table 2 Theoretical relationship of NARMAX model parameter set to continuous-time system coefficients

NARMAX plunge coefficient	Relationship to continuous-time coefficient	NARMAX pitch coefficient	Relationship to continuous-time coefficient
θ_1	$1 - Ta_7$	γ_1	$1 - Tb_8$
θ_2	Ta_1	γ_2	Tb_1
θ_3	Ta_2	γ_3	Tb_2
θ_4	Ta_3	γ_4	Tb_3
θ_5	Ta_4	γ_5	Tb_4
θ_6	Ta_5	γ_6	Tb_5
θ_7	Ta_6	γ_7	Tb_6
θ_8	Ta_8	γ_8	Tb_7
θ_9	Ta_9	γ_9	Tb_9
θ_{10}	$-(1 - Ta_7)$	γ_{10}	$-(1 - Tb_8)$

Table 3 Continuous-time system coefficients

CT coefficient	Value
b	0.135 m
Span	0.600 m
k_h	2844.4 N/M
c_h	27.43 N s/m
ρ	1.225 kg/m^3
c_{l_α}	6.28/rad
c_{l_β}	3.358/rad
c_{m_α}	$(0.5 + a)c_{l_\alpha}$/rad
c_{m_β}	−0.635/rad

Using a fifth-order nonlinearity, the frequency content of the signal at the output of the nonlinearity will be at least 25 Hz (five times the 5-Hz chirp signal). To avoid internal aliasing, a sampling rate of $T = 0.01$ s (100 Hz) is selected, four times greater than the internal 25-Hz signal.

The simulated output $[\hat{y}(n)]$ of the NARMAX description model was compared with the output of the continuous-time simulation $(y(n))$ by computing the percent variance accounted for by the NARMAX model as the percent quality of fit (%QF),

$$\%\text{QF} = \left(1 - \frac{(1/N)\sum_{n=1}^{N}(y(n) - \hat{y}(n))^2}{(1/N)\sum_{n=1}^{N}(y(n))^2}\right) \times 100 \qquad (13)$$

where N is the record length.

B. Simulation Result

This section illustrates the results of simulating the pitch–plunge model in continuous time against the discrete-time NARMAX predictions. Figure 2 shows the simulation input (upper panel) and predicted velocity outputs of the NARMAX description models superimposed on top of the continuous-time outputs of the pitch (lower left panel) and plunge (lower right panel) velocity models. With over 99%QF the NARMAX outputs matched that of the continuous-time simulation with negligible error.

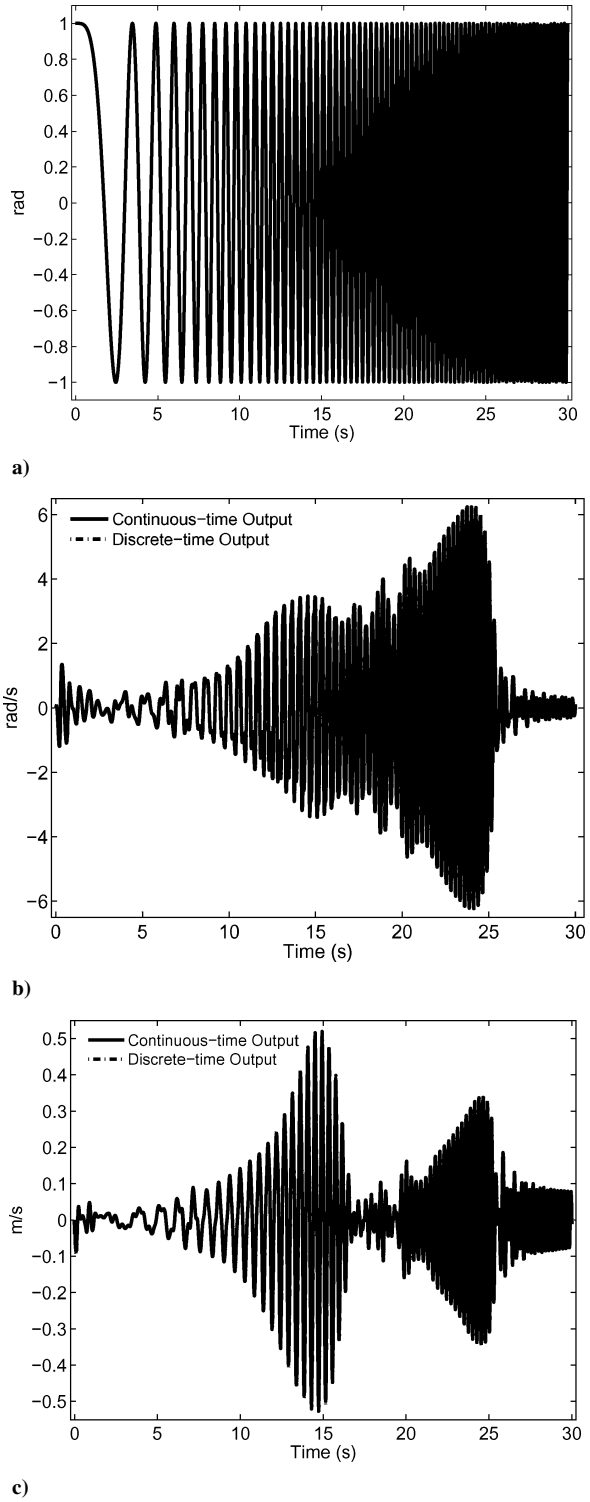

Fig. 2 a) Input to simulated pitch–plunge model in continuous-time and NARMAX description model, b) pitch velocity, and c) plunge velocity output of simulated pitch–plunge velocity model in continuous-time and NARMAX description model (note that the two outputs are almost identical).

VI. NARMAX Identification of Pitch–Plunge Model

We then assessed the utility of methods developed for identifying NARMAX models using sampled data from this continuous-time simulation. An extended least-squares (ELS) algorithm[26–28] was used to identify model parameters.

The NARMAX description of the pitch–plunge velocity models (12) is based on past outputs that are linear in the parameters. In the presence of output additive noise (11) and (12), these terms result in lagged values of disturbance terms that are also linear in the parameters. If these lagged errors are not modeled they induce a bias in the parameter estimates.[24,29,30] The ELS algorithm was implemented because it is designed to model lagged error terms, thereby providing unbiased parameter estimates.

It is well known that ELS may suffer from convergence problems.[24,31,32] However, no prediction error identification method is optimal. For the pitch-plunge velocity models, this is deemed the best estimation technique because it provides an unbiased estimate of model parameters.[24] Other estimation techniques such as

maximum likelihood, instrumental variables, and weighted least-squares are difficult to implement and also have convergence problems.[24,32,33] For this reason ELS is chosen.

A. Analysis of NARMAX Model Parameters

A Monte Carlo study of these NARMAX parameters (Eq. (12) and Table 2) was performed to assess their accuracy and variability using the ELS estimator. One thousand Monte Carlo simulations were generated in which the input–output realization was the same but had a unique Gaussian white, zero-mean noise sequence added to the output. The output additive noise amplitude was increased in increments of 5 dB, from 20 to 0 dB SNR. Parameter mean and standard deviation were computed from the 1000 estimates. The input used for this study was the same 5-Hz chirp signal described in Section V.A.

For this study, the system order and structure were assumed to be known, with the coefficient set in (12) and Tables 2 and 3. The regressor matrix used by this algorithm was formed to contain only those columns (parameters) that corresponded to the theoretical analysis (12). It is reasonable to assume that the order and structure are known because the goal is to identify a model in the model class described by (12).

In experimental settings, often only pitch–plunge displacement and/or acceleration signals are available. For a velocity model description, the velocity signal is required for identification. Therefore, pitch–plunge acceleration signals are numerically integrated to obtain a velocity profile. The estimation set consisted of $N = 3000$ data points sampled at $T = 0.01$ s. The estimated parameters were cross-validated with a fresh noise-corrupted output to compute the %QF of the predicted pitch and plunge velocity. The validation set consisted of $N_v = 3000$ data points.[24,34]

B. Identification Results of Simulated Model

Figure 3 shows the results of identifying this simulated model of pitch–plunge. The NARMAX parameters in this figure correspond to those given in Table 2. This figure shows that the identified parameter values corresponded closely to those derived theoretically for all signal-to-noise ratios (SNR). Note that it is not expected that the mean values of parameters γ_{10} and θ_{10} are close to the theoretically computed value, because they correspond to lagged error terms. Lagged error terms are difficult to identify accurately even with high SNR because they model the output additive noise, which is an unmeasurable stochastic process. This stochastic process is modeled (approximated) by a deterministic signal of prediction errors, which is only a (poor) estimate of the noise.[24,30]

Figure 4 presents a result of cross-validation for a typical parameter set for this study. The top panels show a noise-corrupted output used for identification and the bottom panels show a predicted output superimposed on top of the noise-free output. The predicted output matched the measured output with over 98%QF.

VII. Identification of Experimental Pitch–Plunge Data

Last, the identification technique is assessed on experimental wing section data collected in the wind tunnel at the Department of Aerospace Engineering, Texas A&M University, by the Aeroelasticity Research Group. The data analyzed for this study did not contain a flap control input but instead had an initial condition associated

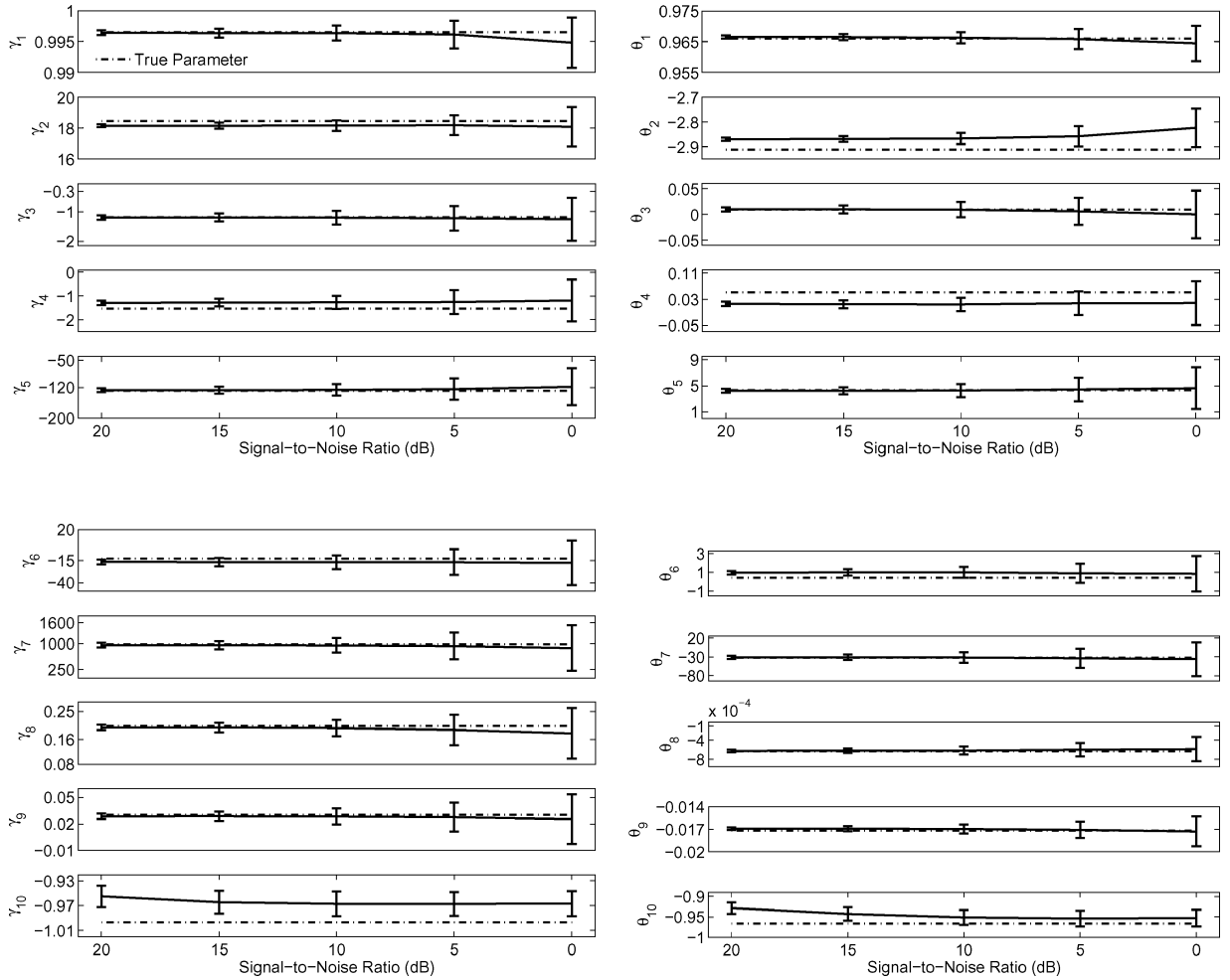

Fig. 3 Monte Carlo study of pitch–plunge NARMAX model parameters. Pitch parameters (left): Mean and STD. Plunge parameters (right): Mean and STD. 5 Hz chirp input, Gaussian, white, zero-mean noise and N = 3000. Ordinate: STD about mean. Abscissa: Output SNR = 20, 15, 10, 5 and 0 dB. (Note that the abscissa is shown in decreasing SNR which corresponds to increasing noise intensity.)

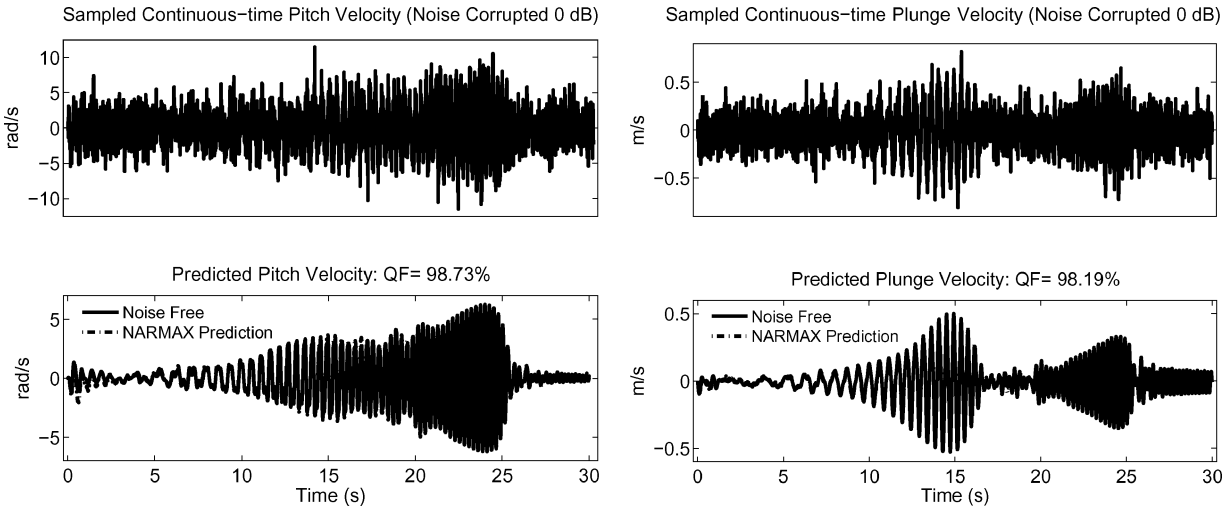

Fig. 4 Cross-validation for typical identified NARMAX pitch (left) and plunge (right) models with $N_v = 3000$ and Gaussian, white, zero-mean output additive noise (0 dB SNR). Top panels: Measured outputs used for estimation. Bottom panels: Predicted output superimposed on top of noise-free output.

with plunge displacement. Data with a control input were unavailable for analysis.

The velocity model descriptions given in Eq. (12) are in terms of a control input and zero initial conditions. For the present study the model was modified to reflect a lack of exogenous input and the presence of an initial condition. Model 12 is reformulated as

$$\begin{aligned}\dot{h}(n) &= \theta_1\dot{h}(n-1) + \theta_2 h(n-1) + \theta_3\alpha(n-1) + \theta_4\alpha(n-1)^2 \\ &\quad + \theta_5\alpha(n-1)^3 + \theta_6\alpha(n-1)^4 + \theta_7\alpha(n-1)^5 + \theta_8\dot{\alpha}(n-1) \\ &\quad + \theta_9\delta(n) + \theta_{10}e_{\dot{h}}(n-1) \\ \dot{\alpha}(n) &= \gamma_1\dot{\alpha}(n-1) + \gamma_2 h(n-1) + \gamma_3\alpha(n-1) + \gamma_4\alpha(n-1)^2 \\ &\quad + \gamma_5\alpha(n-1)^3 + \gamma_6\alpha(n-1)^4 + \gamma_7\alpha(n-1)^5 \\ &\quad + \gamma_8\dot{h}(n-1) + \gamma_9 e_{\dot{\alpha}}(n-1) \qquad (14)\end{aligned}$$

where $\delta(n)$ is the Kronecker impulse function used to represent the onset of a plunge initial condition in discrete time. Note that this model description can also be modified for use in analysis of data that contain both an initial condition and exogenous input, by simply including a Kronecker impulse function in Eq. (12), or neither (time-series analysis), by removing the exogenous input term.

A. Apparatus

Data were collected in a unique wind-tunnel test apparatus at the Department of Aerospace Engineering, Texas A&M University. This $2' \times 3'$ closed-circuit low-speed wind tunnel allows a wing section to move in two degrees of freedom and can translate (plunge) and rotate (pitch). This apparatus allows the study of classical bending–torsion flutter. Structural response of the system is governed by springs attached to cams. Stiffness of the springs and shape of the cams can be altered to prescribe a wide variety of linear and nonlinear structural responses.

B. Procedures

The pitch acceleration was measured by a linear accelerometer, which measured accelerations along one axis. The accelerometer was mounted 0.157 m from the rotational axis and orthogonal to the y-direction when the airfoil was at a zero angle of attack, giving no acceleration in the y-direction. However, a small portion of plunge acceleration was detected when the airfoil was deflected. The elastic axis was 3/10 of the chord length forward of the midchord.

The freestream velocity was increased in increments of 2 m/s, from 4 to 22 m/s. Aeroelastic responses were recorded for 45 s while the free stream velocity was held constant. Flutter was observed to be induced at about 13.5 m/s. Pitch and plunge displacements and accelerations of this aeroelastic system were sampled at 525 Hz.

After recording, the experimental data was resampled by a factor of 2, resulting in a final sampling rate of 262.5 Hz. The system was identified using the NARMAX approach, as outlined in Section VII.A, except that $N = 15{,}600$ points was used for estimation and $N_v = 7{,}800$ points was used for validation.

C. Results

The results of identifying 10 trials of wing section experiments are presented. Figures 5a and 5b show a typical pitch–plunge displacement and velocity trial used for this analysis.

The data represent pitch and plunge displacement and velocity sequences when the free stream velocity in the wind tunnel was held constant at 16 m/s. The characteristics of this trial are consistent with those reported in previous work.[35] Figures 5c and 5d display a 5-s slice of the cross-validation (predicted) outputs superimposed on top of the measured outputs for this trial. The predicted outputs matched the measured outputs with over 98%QF.

Figure 6 shows the cross-validation %QF for each trial. The results show that the predicted outputs for these parameter estimates account for a large portion of the variance. For pitch velocity, the range of %QF is from a minimum of 99.73% to a maximum of 99.98%. For plunge velocity, the range of %QF is from a minimum of 98.09% to a maximum of 99.83%. From the 10 trials examined for this study, 80% of predicted outputs accounted for more than 99%QF of the measured output for both pitch and plunge velocity. This indicates that the NARMAX parameters explain the measured data well. Moreover, for every data set the standard deviation (STD) of each model parameter was computed at the 95% confidence level. These results showed that the STDs did not contain zero. This suggests that the estimated models are accurate. A model parameter the STD of which encompasses zero may indicate a spurious model term and, hence, should be reformulated.[36]

VIII. Discussion

A. NARMAX Representation of Pitch–Plunge Velocity Dynamics

The theoretical results demonstrate that the nonlinear difference equation description for the pitch–plunge models is a NARMAX model. Simulation results show that the NARMAX models match the continuous-time response well. This suggests that parametric nonlinear model forms such as the NARMAX class can be used for modeling aerospace systems.

Nonlinear models have the advantage that they cover a wider range of system dynamics than linear models, which could allow faster envelope expansion. Using LTI models for envelope expansion, the dynamics need to be reestimated as, for example,

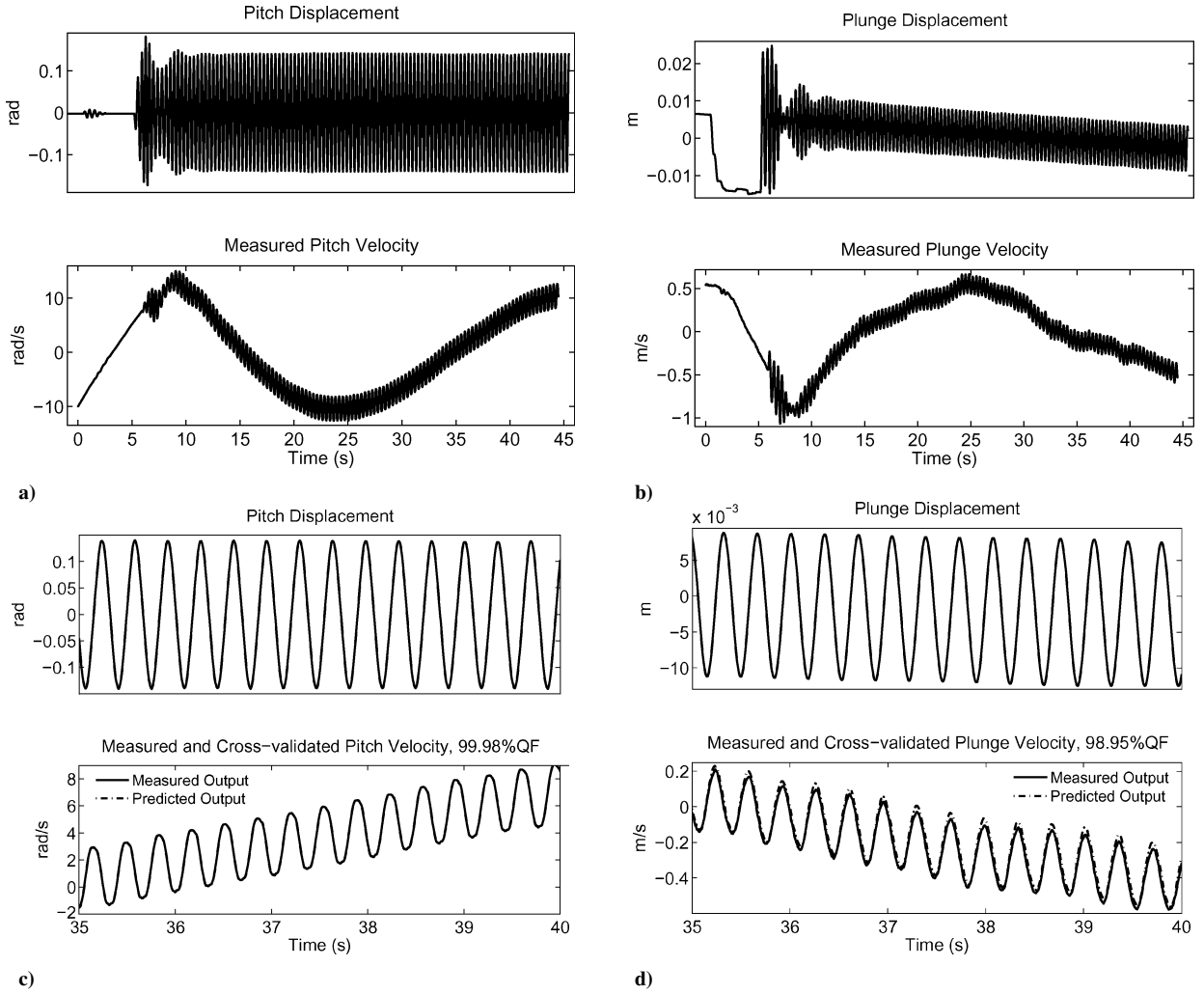

Fig. 5 a) and b) Typical recorded pitch and plunge displacement and velocity. c) and d) Cross-validation. Upper panels: 5-s slice of pitch and plunge displacement. Lower panels: 5-s slice of predicted pitch and plunge velocity outputs superimposed on top of measured velocity output for identified NARMAX pitch–plunge velocity models for experimental data set with $Nv = 7800$.

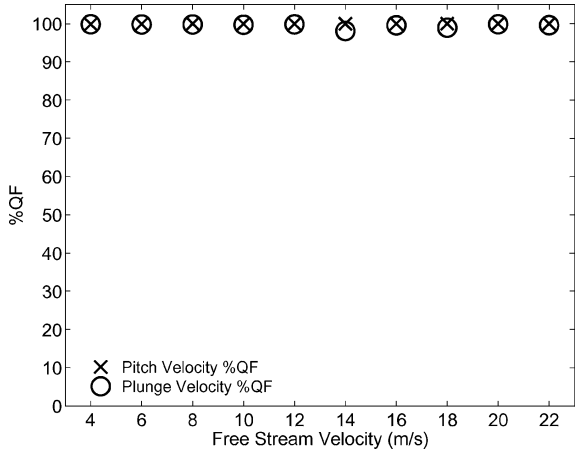

Fig. 6 Cross-validation: %QF versus freestream velocity (experimental trial).

the freestream velocity changes. This is because, as the freestream velocity varies, the system will operate over a different region of the nonlinearity. With nonlinear identification, the model and, hence, its parameters are valid over a larger operating regime, because it explicitly accounts for nonlinear effects.[24] These nonlinear effects are modeled as nonlinear input–output terms [see Eqs. (1) and (12)]. Identification of nonlinear models, which are linear in the parameters, is more efficient than developing a set of LTI models, which may be valid over only a small operating region. With a NARMAX approach, only one model is needed to describe the complex underlying dynamics, as opposed to possibly many LTI models, over a given operating regime. Using nonlinear models to characterize aeroelastic phenomena can provide significant time and cost savings for test and development of aerospace vehicles. Moreover, the discrete nonlinear models of pitch–plunge provide excellent predictions, which could be used for control synthesis, and statistical studies of NARMAX coefficients may be of direct relevance for health monitoring of aerostructures.

B. Discrete-Time Parameter Estimation of Simulated Aeroelastic System

Simulation studies in Section VIII.A showed that, for a NARMAX model representation, the mean of Monte Carlo estimates for NARMAX parameters matched the theoretical values well for all SNR levels. However, estimates of some parameters, e.g., γ_{10}, did not correspond well to theoretically computed values. As stated earlier, lagged error terms are difficult to identify accurately. Error terms represent a stochastic process that cannot be measured. This stochastic process is approximated by a deterministic signal of prediction errors, which is only a (poor) estimate of the noise.[24,30]

C. Identification of Experimental Aeroelastic Data

High %QF cross-validation fits obtained for parameter estimates using NARMAX identification methods (see Fig. 6) show that the identified parameters explain the experimental data well. Using %QF alone as an indicator of model goodness may lead to incorrect

interpretations of model validity. However, in many cases, for nonlinear models, this may be the only indicator that is readily available.

A model validation technique for nonlinear systems, using higher-order correlations, was developed by Billings and Voon.[37,38] Korenberg and Hunter[39] showed that this model validation technique fails for simple cases. Therefore, this approach was not implemented, in favor of using the %QF alone as an indicator of model goodness.

In studying aeroelastic systems it may not be practical to assume that the exact model order and structure are well known a priori. In aerospace systems analysis one of the main objectives is not only to estimate system parameters but to gain insight into the structure of the underlying system. It would be worthwhile in a future study to investigate what happens if NARMAX structure detection methods[36,40–42] are allowed to analyze the data to find the best structure from the data set. This may then indicate deficiencies in the analytical model and could lead to improved modeling strategies.

IX. Conclusions

Theoretical results demonstrate that the nonlinear difference equation description for the pitch–plunge model is a NARMAX model. Simulation results show that the NARMAX model matches the continuous-time response well. Moreover, this paper contributes to the understanding of the use of parametric identification techniques for modeling of nonlinear aerospace systems. The main point here is that the NARMAX form is clearly amenable to the study of a wide range of aerospace systems, and could be computationally efficient. NARMAX modeling and identification techniques should be examined further, especially in the case of severe nonlinear behavior.

Acknowledgments

This research was supported by grants from the National Academy of Sciences and NASA Dryden Flight Research Center, Aerostructures Branch (Grant NASA-NASW-99027). The authors dedicate this work in loving memory of Margherita B. Rapagna (Aug. 25, 1968–May 20, 2002).

References

[1]Lee, B., Pricei, S., and Wong, Y., "Nonlinear Aeroelastic Analysis of Airfoils: Bifurcation and Chaos," *Progress in Aerospace Sciences*, Vol. 35, No. 3, 1999, pp. 205–334.

[2]Mukhopadhyay, V., "Historical Perspective on Analysis and Control of Aeroelastic Responses," *Journal of Guidance, Control, and Dynamics*, Vol. 26, No. 5, 2003, pp. 673–684.

[3]Mukhopadhyay, V., "Flutter Suppression Control Low Design and Testing for the Acting Flexible Wing," *Journal of Aircraft* (Special Adaptive Flexible Wing Issue), Vol. 32, No. 1, 1995, pp. 45–51.

[4]Bunton, R., and Denegri, C., "Limit Cycle Oscillation Characteristics of Fighter Aircraft," *Journal of Aircraft*, Vol. 37, No. 5, 2000, pp. 916–918.

[5]Chen, P., Sarhaddi, D., and Liu, D., "Limit Cycle Oscillation Characteristics of Fighter Aircraft with External Stores," AIAA Paper 98-1967, April 1998, p. 1727.

[6]Denegri, C., "Limit Cycle Oscillation Flight Test Results of a Fighter with External Stores," *Journal of Aircraft*, Vol. 37, No. 5, 2000, pp. 761–769.

[7]Greblicki, W., and Pawlak, M., "Nonparametric Identification of a Cascade Nonlinear Time Series System," *Signal Processing*, Vol. 22, No. 1, 1991, pp. 61–75.

[8]Kosut, R., Lau, M., and Boyd, S., "Set-Membership Identification of Systems with Parameteric and Nonparametric Uncertainty," *IEEE Transactions on Automatic Control*, Vol. 37, No. 7, 1992, pp. 929–942.

[9]Masri, S., and Caughey, T., "A Nonparametric Identification Technique for Nonlinear Dynamic Problems," *Journal of Applied Mechanics*, Vol. 46, No. 2, 1979, pp. 433–447.

[10]Lind, R., Prazenica, R., and Brenner, M., "Estimating Nonlinearity Using Volterra Kernals in Feedback with Linear Models," *Nonlinear Dynamics*, Vol. 39, No. 1, 2005, pp. 3–23.

[11]Leontaritis, I., and Billings, S., "Input–Output Parametric Models for Non-linear Systems. Part I: Deterministic Non-linear Systems," *International Journal of Control*, Vol. 41, No. 2, 1985, pp. 303–328.

[12]Leontaritis, I., and Billings, S., "Input–Output Parametric Models for Non-linear Systems. Part II: Stochastic Non-linear Systems," *International Journal of Control*, Vol. 41, No. 2, 1985, pp. 329–344.

[13]Billings, S., and Chen, S., "Extended Model Set, Global Data and Threshold Model Identification of Severely Non-linear Systems," *International Journal of Control*, Vol. 50, No. 5, 1989, pp. 1897–1923.

[14]Chen, S., and Billings, S., "Representations of Non-linear Systems: The NARMAX Model," *International Journal of Control*, Vol. 49, No. 3, 1989, pp. 1013–1032.

[15]Chen, S., Billings, S., Cowan, C., and Grant, P., "Practical Identification of NARMAX Models Using Radial Basis Functions," *International Journal of Control*, Vol. 52, No. 6, 1990, pp. 1327–1350.

[16]Kukreja, S., Galiana, H., and Kearney, R., "NARMAX Representation and Identification of Ankle Dynamics," *IEEE Transactions on Biomedical Engineering*, Vol. 50, No. 1, 2003, pp. 70–81.

[17]O'Neil, T., and Strganac, T. W., "Nonlinear Aeroelastic Response—Analyses and Experiments," AIAA Paper 96-1390, April 1996, p. 0014.

[18]O'Neil, T., Gilliatt, H. C., and Strganac, T. W., "Investigations of Aeroelastic Response for a System with Continuous Structural Nonlinearities," AIAA Paper 96-1390, April 1996, p. 1390.

[19]Dowell, E., "Nonlinear Aeroelasticity," *Structures, Structural Dynamics, and Materials Conference*, Vol. 31, 1990, pp. 1497–1509.

[20]Tang, D., and Dowell, E., "Flutter and Stall Response of a Helicopter Blade with Structural Nonlinearity," *Journal of Aircraft*, Vol. 29, 1990, pp. 953–960.

[21]Yang, Z., and Zhao, L., "Analysis of Limit Cycle Flutter of an Airfoil in Incompressible Flow," *Journal of Sound and Vibration*, Vol. 123, No. 1, 1988, pp. 1–13.

[22]Zhao, L., and Yang, Z., "Chaotic Motions of an Airfoil with Nonlinear Stiffness in Incompressible Flow," *Journal of Sound and Vibration*, Vol. 138, No. 2, 1990, pp. 245–254.

[23]Franklin, G., Powell, J., and Emami-Naeini, A., *Feedback Control of Dynamic Systems*, 4th ed., Addison–Wesley, New York, 2002.

[24]Ljung, L., *System Identification: Theory for the User*, 2nd ed., Prentice–Hall, Englewood Cliffs, NJ, 1999.

[25]Åström, K., *Computer-Controlled Systems: Theory and Design*, 3rd ed., Prentice–Hall, Upper Saddle River, NJ, 1997.

[26]Panuska, V., "A Stochastic Approximation Method for Identification of Linear Systems Using Adaptive Filtering," *Proceedings 9th Joint Automatic Control Conference*, IEEE, Piscataway, NJ, 1968, pp. 1014–1021.

[27]Panuska, V., "An Adaptive Recursive Least Squares Identification Algorithm," *Proceedings 8th IEEE Symposium on Adaptive Processes*, Piscataway, NJ, Nov. 1969, paper 6e.

[28]Young, P., "The Use of Linear Regression and Relaxed Procedures for the Identification of Dynamic Processes," *Proceedings 7th IEEE Symposium on Adaptive Processes*, Piscataway, NJ, Dec. 1968, pp. 501–505.

[29]Billings, S., and Voon, W., "Least Squares Parameter Estimation Algorithms for Non-linear Systems," *International Journal of Systems Science*, Vol. 15, No. 6, 1984, pp. 601–615.

[30]Goodwin, G., and Payne, R., *Dynamic System Identification: Experiment Design and Data Analysis*, Mathematics in Science and Engineering, Vol. 136, Academic Press, New York, 1977.

[31]Walter, E., and Pronzato, L., *Identification of Parametric Models*, 1st ed., Springer-Verlag, Berlin, 1997.

[32]Söderström, T., and Stoica, P., *System Identification*, Prentice–Hall, Upper Saddle River, NJ, 1989.

[33]Stoica, P., and Söderström, T., "Asymptotic Behavior of Some Bootstrap Estimators," *International Journal of Control*, Vol. 33, No. 3, 1981, pp. 433–454.

[34]Shao, J., "Linear Model Selection by Cross-Validation," *Journal of the American Statistical Association*, Vol. 88, No. 422, 1993, pp. 486–494.

[35]Kurdila, A., Prazenica, R., Rediniotis, O., and Strganac, T., "Multiresolution Methods for Reduced-Order Models for Dynamical Systems," *Journal of Guidance, Control, and Dynamics*, Vol. 24, No. 2, 2001, pp. 193–200.

[36]Kukreja, S., Galiana, H., and Kearney, R., "A Bootstrap Method for Structure Detection of NARMAX Models," *International Journal of Control*, Vol. 77, No. 2, 2004, pp. 132–143.

[37]Billings, S., and Voon, W., "Structure Detection and Model Validation Tests in the Identification of Nonlinear Systems," *IEE Proceedings, Part D, Control Theory and Applications*, Vol. 130, No. 4, 1983, pp. 193–199.

[38]Billings, S., and Voon, W., "Correlation Based Model Validity Tests for Non-linear Models," *International Journal of Control*, Vol. 44, No. 1, 1986, pp. 235–244.

[39]Korenberg, M., and Hunter, I., "The Identification of Nonlinear Biological Systems: Wiener Kernel Approaches," *Annals of Biomedical Engineering*, Vol. 18, 1990, pp. 629–654.

[40]Korenberg, M., "Orthogonal Identification of Nonlinear Difference Equation Models," *Proceedings of the Midwest Symposium on Circuit Theory*, Vol. 1, IEEE Publications, Piscataway, NJ, 1985, pp. 90–95.

[41]Korenberg, M., Billings, S., Liu, Y., and McIlroy, P., "Orthogonal Parameter Estimation Algorithm for Nonlinear Stochastic Systems," *International Journal of Control*, Vol. 48, No. 1, 1988, pp. 193–210.

[42]Kukreja, S., Kearney, R., and Galiana, H., "A Bootstrap Method for NARMAX Model Order Selection," *Proceedings of the 4th IFAC Symposium on Modelling and Control in Biomedical Systems*, Vol. 4, International Federation of Automatic Control, Laxenburg, Austria, 2000, pp. 353–356.